Article

Less impact of limestone bedrock on elemental concentrations in stream sediments – Case study of Akiyoshi area –

Atsuyuki Ohta[1, *] and Masayo Minami[2]

Abstract: Geological survey of Japan, National Institute of Advanced Industrial Science and Technology has created the nationwide geochemical maps of 53 elements using fine stream sediments (< 180 μm) in Japan. The spatial distribution patterns of elemental concentrations of stream sediments reflect faithfully the distribution of geology and mineral deposits. However, the exception is limestone bedrock, which insignificantly influences on elemental concentrations of stream sediments. To clarify the reason, we collected stream sediments from Akiyoshi-dai, where is underlain by the largest-scale limestone bedrock. Fine stream sediments (< 180 μm), whose drainage basins are occupied by limestones, have high CaO and Sr concentrations and intensive peak of calcite obtained by X-ray diffractometry. Examining variation of elemental concentrations against the particle size of sediments, the finer particle contains a higher proportion of calcite and has higher CaO concentration. However, CaO concentration (10–20 wt. %) in stream sediments is much lower than expected values (~50%); nevertheless limestone outcrops in more than 70 % in their watersheds. The contradictory finding is explained by less contribution of limestone clastics to river system because limestone bedrocks are easily dissolved by water (chemical weathering) but not susceptible to physical weathering and erosion process. In other words, the supply quantity of clastic materials from limestone bedrocks is much smaller than those of other rock types. In addition, Sr concentration in some samples does not correlate with either CaO concentration or the peak intensity of calcite; nevertheless Sr is expected to have similar chemical properties to CaO. The fact suggests that calcite formed from water oversaturated for calcium carbonate is supplied to river system; it has the different Sr concentrations from Akiyoshi Limestone.

Keywords: Akiyoshi-dai; limestone; stream sediment; geochemical map; calcium; strontium

1. Introduction

The Geological Survey of Japan, National Institute of Advanced Industrial Science and Technology prepared nationwide geochemical maps of 53 elements in stream sediments for environmental assessment (Imai *et al*., 2004). Stream sediments are considered to be a composite sample of the products of weathering and erosional of soil and rocks in the catchment area upstream from the sampling site (Howarth and Thornton, 1983). In other words, the spatial distribution patterns of elemental concentrations are controlled conclusively by parent lithology and mineral deposits. Ohta *et al*. (2004a, 2004b, 2005) revealed that this assumption is also reasonable in Japan, where geology has particularly complicated distributions and many mineral deposits occur on a small

scale. However, ultramafic rock and limestone associated with accretionary complexes were exceptions. Ultramafic rock elevates highly MgO, Cr, Co, and Ni concentrations in stream sediments, even if it crops out only in a small area (Ohta *et al*., 2004b, 2005). Meanwhile, the contribution of limestone for elemental concentrations in stream sediments was very small in Japan. The stream sediments derived from accretionary complexes associated with a large-scale limestone bedrock were significantly poor in CaO and Sr than other sediments (Ohta *et al*., 2004a). In European countries, extremely high CaO concentration (10–55%) in stream sediments found in the area covered by calcareous sediments and limestone (e.g., De Vos *et al*., 2006; Albanese *et al*., 2007). The sampling density of Japanese geochemical mapping project is low: 1 site per 100 km^2 (Imai *et al*., 2004). Japanese limestone is

[1]AIST, Geological Survey of Japan, Institute of Geology and Geoinformation

[2]Center for Chronological Research, Nagoya University, Chikusa, Nagoya 464-8602, Japan

*Corresponding author: A. OHTA, Central 7, 1-1-1 Higashi, Tsukuba, Ibaraki 305-8567, Japan. E-mail a.ohta@aist.go.jp
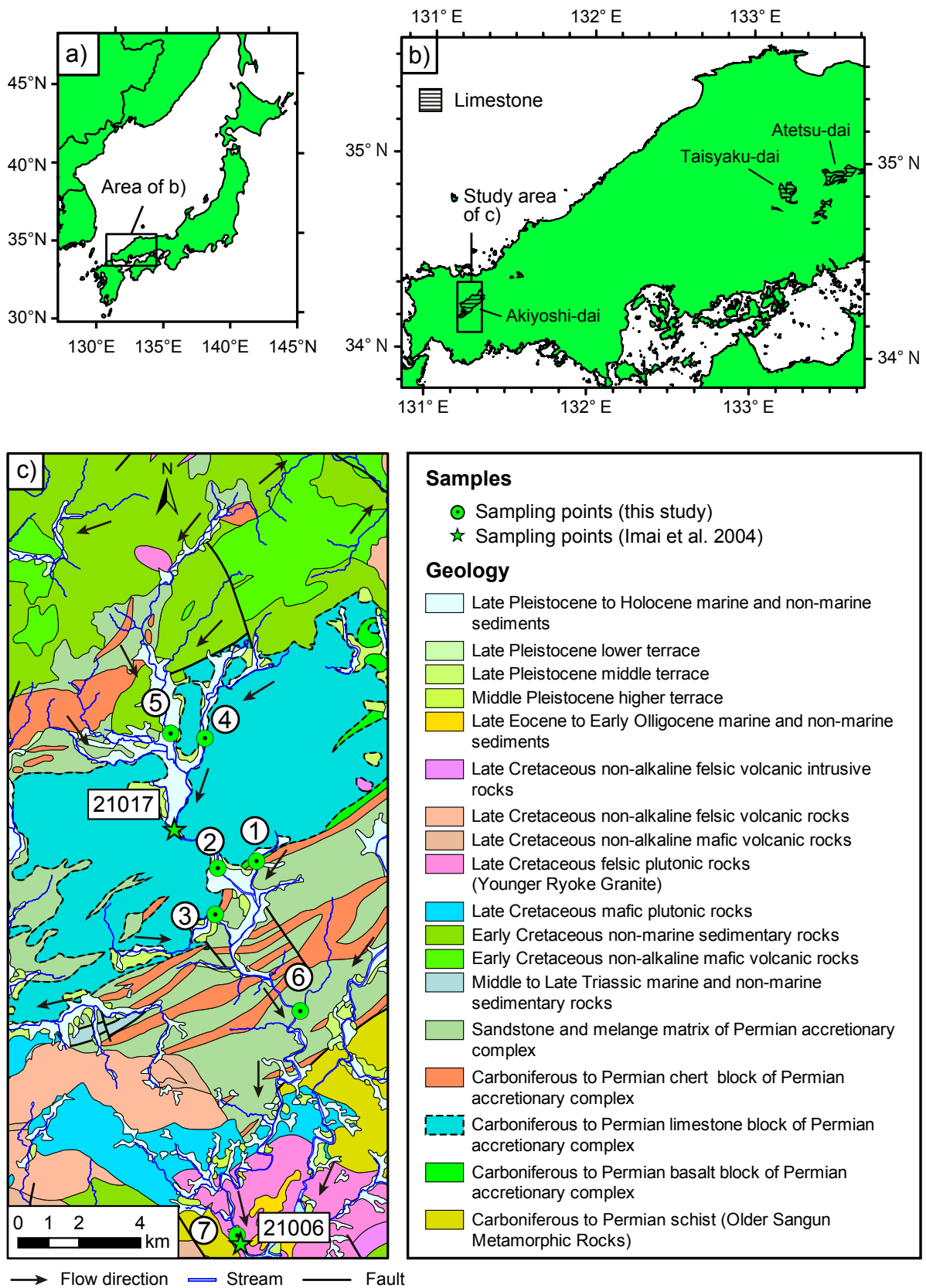
Fig 1. a) Schematic map of the study area. b) Chugoku region with large-scale limestone bedrocks (Akiyoshi-dai, Taisyaku-dai and Atetsu-dai). c) Geological map around the Akiyoshi-dai at a scale of 1:200,000 (Matsuura *et al.*, 2007; Geological Survey of Japan, AIST, 2012).

Table 1.   Relative ratio by weight of respective grain sizes to sediments less than 2 mm.

Grain size	Akiyoshi						
	1	2	3	4	5	6	7
<180 μm	4.5%	3.6%	6.4%	4.2%	6.1%	4.9%	22%
1-2 mm	33%	43%	41%	42%	31%	42%	12%
500–1000 μm	28%	29%	27%	23%	34%	24%	15%
250–500 μm	25%	19%	19%	23%	24%	26%	21%
125–250 μm	9.2%	6.5%	8.1%	8.5%	8.5%	5.1%	22%
63–125 μm	2.3%	1.2%	3.1%	2.1%	1.9%	1.1%	19%
32–63 μm	0.9%	0.6%	1.1%	1.4%	0.7%	0.8%	8.2%
<32 μm	0.6%	0.6%	0.4%	0.4%	0.3%	0.7%	3.2%

small in size and distributes sporadically. Therefore small limestone-exposed area in watershed might be the reason why the less influence of limestone on elemental concentrations in stream sediments (Ohta *et al*., 2004a). To elucidate the particle transfer process in limestone region, we focus on the Chugoku region where large-scale limestone bedrocks (Akiyoshi-dai, Taisyaku-dai and Atetsu-dai) are exposed (Fig. 1a and b).

2. Study area and samples

2.1 Geology

Figure 1c depicts the geology at a 1:200,000 scale (Matsuura *et al*. 2007; Geological Survey of Japan, 2012). The central part of the study area is covered by Permian accretionary complexes consisting of trench fills (sandstone and mélange matrix) and exotic blocks of oceanic rocks, chert, limestone and metabasalt that range in age mainly through the Carboniferous–Permian. The Akiyoshi Limestone is originated from a Carboniferous-Permian atoll complex upon a seamount (Sano and Kanmera, 1991). They consist of heterogeneous aggregate of the collapsed product during the subducting process in the Middle Permian (Sano and Kanmera, 1991): a complicated mixture of limestone and metabasalt blocks. A surface part of them is covered thinly by the Late Pleistocene to Holocene sediments. Cretaceous non-marine sedimentary rocks (red shale, sandstone, and conglomerate) and Cretaceous basaltic–andesitic lava and tuff are distributed in the northern and southern parts. Rhyolite-dacitic tuffacious rocks cropout in the northeastern and southwestern part. Granitic rocks intruded during Cretaceous time occur mainly in southern part and sporadically in the northern part. High-pressure typed metamorphic rocks distributing on the southeastern side consist mainly of pelitic schist.

2.2 Samples

The Akiyoshi-dai is selected for the study area; stream sediment samples were collected in the high density (Fig. 1c). All samples were collected from the Kotou river

system flowing through the Akiyoshi Limestone bedrock. Samples nos. 1, 3, 4, and 5 were collected from the subsidiary stream; samples nos. 2, 6, and 7 were collected from the main river (Fig. 1c). The river sediments at the locations nos. 1 and 3 consisted dominantly of fine sandy sediments. The riverbeds at the locations nos. 2, 4, 5, and 6 were covered by coarse sediment including cobbles and gravels. Especially the riverbed at the location no. 6 was covered dominantly by cobbles and gravels: sandy sediments deposited among them were collected. The location no. 7 is situated at the upper reach of the dam lake. The very fine sandy and silty sediments were deposited there. The star symbols indicate the samples (nos. 21006 and 21017) collected for the nationwide Japanese geochemical mapping (Imai *et al*., 2004).

The collected samples were dried in air and sieved with a 180 μm screen for comparison with the data of Japanese geochemical maps. The duplicated sample was sieved with 7 kinds of screens: 2 mm, 1 mm, 500 μm, 250 μm, 125 μm, 63 μm, and 32 μm screens. The coarser grains over 2 mm were not used for the study. The sieved samples were ground with an agate mortar and pestle. Table 1 summarized the relative ratio by weight of respective grain sizes to samples sieved with 2 mm. The relative ratio by weight of <180 μm is about 4–6% for most cases, but is extremely high for sample no. 7 (22%). Those values do not correlate to a respective catchment area. The 80–90% of stream sediments less than 2 mm is composed of medium to very coarse-grained sands (over 250 μm). However, the coarse sands of sample no. 7 account for just 48% of total sediments sieved with a 2 mm screen. The percentages of fine sands and silty grains (less than 250 μm) of sample no. 7 are extremely higher than those of the other samples.

3. Analytical methods

The degradation of samples follows the method used in Japanese geochemical mapping project (Imai *et al*., 2004). 0.2 g of each sample was digested using HF (5 ml), HNO_3 (3 ml) and $HClO_4$ (2 ml) at 120°C for 3 hr.
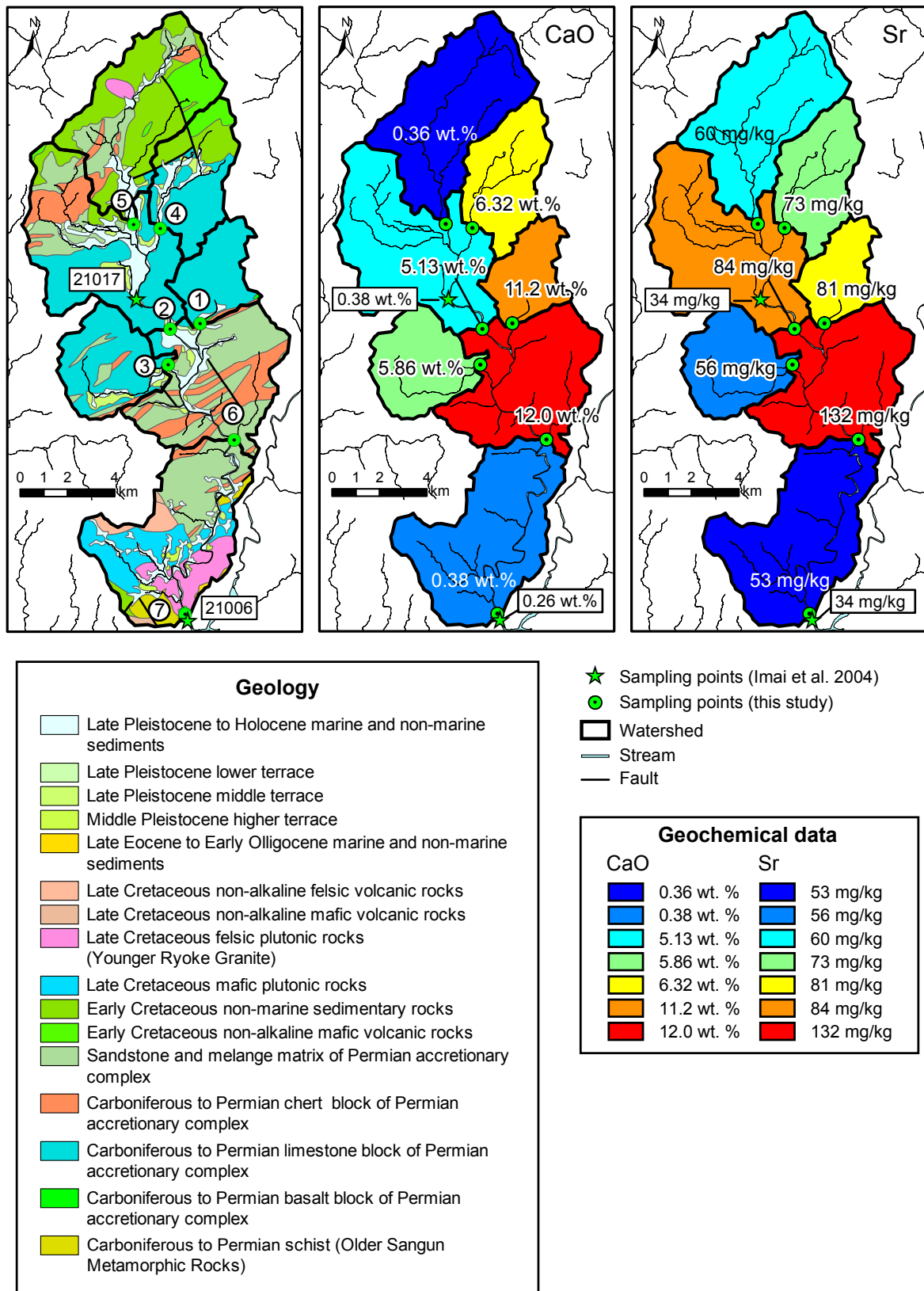
Fig 2. Catchment areas including geology at a scale of 1:200,000 (Matsuura *et al*., 2007; Geological Survey of Japan, AIST, 2012), and CaO and Sr concentrations of stream sediments sieved with a 180 μm screen.

The degraded product was evaporated to dryness under 180°C and the residue was dissolved with 5 ml of 7 mol/L HNO_3. The dissolved solution was diluted to be 100 mL with deionized water. Concentrations of 51 elements were determined using: ICP-AES (Na_2O, MgO, Al_2O_3, P_2O_5, K_2O, CaO, TiO_2, MnO, Total (T-) Fe_2O_3, V, Sr, and Ba) and ICP-MS (Li, Be, Sc, Cr, Co, Ni, Cu, Zn, Ga, Rb, Y, Zr, Nb, Mo, Cd, Sn, Sb, Cs, La, Ce, Pr, Nd, Sm, Eu, Gd, Tb, Dy, Ho, Er, Tm, Yb, Lu, Hf, Ta, Tl, Pb, Bi, Th, and U). Table 2 summarizes analytical results for the stream sediments.

The samples were further characterized using x-ray powder diffraction (XRD) with CuKα radiation (RIGAKU RINT-2500). The x-ray tube was operated at 40 kV with a 100 mA current. The scanning velocity was 2°(2θ)/min. Sample was placed in a reflection free sample holder (15 mm × 20 mm × 0.2 mm) and pressed vertically using a microscope slide glass to planarize the surface and removed excess sample powders.

4. Results

4.1 Watershed analysis

To elucidate the dominant lithology distributing in respective river system, the watershed stream network was calculated from the digital elevation model (50 m mesh data) provided by the Geographical Survey Institute, Japan. The GIS software (ArcGIS 10.0; Environmental Systems Research Institute) was used for the calculation. Figure 2 portrays the catchment boundary obtained for each sampling location. The area of estimated watershed boundary is summarized in Table 3. The area of watershed of samples nos. 1, 3, 4, and 5 are 10–30 km². Those sampling density is 3–10 times as high as those of Japanese geochemical mapping project (1 sample/100 km²). The catchment areas for samples nos. 2, 6, and 7 include those for samples collected upper stream: these determined areas range from 78 km² to 164 km².

We assumed that elemental concentrations of stream sediments are determined by the representative lithology, which is the specific rock type exposed in a drainage basin most widely. The intended lithology was Pleistocene-Holocene unconsolidated sediments, Cretaceous sedimentary rocks, Permian accretionary complexes, Cretaceous felsic and mafic volcanic rocks, Cretaceous felsic and mafic plutonic rocks and Carboniferous to Permian metamorphic rocks (mainly pelitic schist). Permian accretionary complexes are further grouped into four: sandstone-mélange matrix, limestone, chert and metabasalt. Table 3 summarizes the relative exposed areas of these lithologies in each drainage basin. Limestone is the dominant lithology in the catchment areas for samples nos. 1, 3, and 4. Pleistocene to Holocene sediments, Cretaceous sedimentary rocks, sandstone and mélange matrix of Permian accretionary complexes are distributed in the watershed of samples nos. 2, 5, 6, and 7. The volcanic, plutonic and metamorphic rocks are the minor lithologies in watershed area of all samples. Table 3 suggests that all samples except for no. 5 contain

limestone bedrocks in their river basins. For comparison, the watershed analysis result for samples nos. 21006 and 21017 were also shown in Table 3. The catchment area of sample no. 21006 includes that of 21017. A quarter of those watersheds is covered by limestone bedrocks.

4.2 Spatial distribution patterns of elemental concentrations in stream sediments

Figure 2 portrays the catchment areas, geology within respective watersheds, and CaO and Sr concentrations of stream sediments sieved with 180 μm in order to visualize the relationships between geology and CaO (or Sr) concentration. Five samples out of the newly corrected seven samples have high CaO concentration (5–12 wt. %). However, those values are much lower than 53–55 wt. % of CaO concentration in pure limestone. Sample no. 5 has low CaO concentration (0.36 wt. %) because little limestone distributes in its river basin, where sandstone and mélange matrix of Permian accretionary complexes, Cretaceous sedimentary rocks and Cretaceous mafic volcanic rocks are exposed (Fig. 2a and Table 3). Although sample no. 21017 locates just two km upstream from sample no. 2, its CaO content is no more than 0.38 wt. %. Sample no. 6 has the highest CaO concentration (12.0 wt. %) among 7 samples. Sandstone and chert of Permian accretionary complexes distribute widely around the location no. 6. The fact indicates that calcareous sediment is indeed conveyed from upstream to location no. 6. The samples nos. 7 and 21006 present in the lowest reaches of the Kotou River. Both samples have the quite low CaO concentration, nevertheless their drainage basin contains limestone bedrock as in the case with sample no. 6. The Sr concentration of stream sediments collected in river system underlain by limestone is high (73–132 mg/kg) in analogy with CaO concentration. As exception, Sr content in sample no. 3 is as low as those of samples nos. 5, 21006, and 21017. The Sr concentration of the Akiyoshi Limestone is 80–340 mg/kg (Nakano and Ishihara, 2003). The Sr concentration of stream sediments is somewhat lower than that of limestone bedrocks.

Next, we examined the features of concentrations of the other elements (Table 2). Little variation is observed for Al_2O_3 concentration among seven samples. The samples nos. 1 and 3 have low concentrations of Na_2O, K_2O, Rb, Ba and high concentrations of P_2O_5, TiO_2, T-Fe_2O_3, V, Cr, Co, Ni, Cu, Zn, Y, and lanthanide (La–Lu). The high concentrations of P_2O_5 and 3d transition elements in samples nos. 1 and 3 would be caused by metabasalt associated with the Akiyoshi Limestone (Figs. 1c and 2). The samples nos. 5 and 7 have high K_2O, Rb and Ba concentrations; low MnO and rare earth element concentrations.

4.3 Variation of elemental concentrations in stream sediments according to grain size

Figure 3 shows how CaO and Sr concentrations in stream sediments change according to grain size. Samples nos. 1, 2, 3, 4, and 6 whose CaO concentration is high,

Table 2. Analytical results of fine stream sediments (<180 μm) collected from the Kotou River and those derived from sedimentary rocks in accretionary complexes in Chugoku region.

| | | Akiyoshi (this study) | | | | | | | Imai et al. (2004)[a] | | Ohta et al. (2004)[b] |
		1	2	3	4	5	6	7	21006	21017	Med. (min. ~ max.)
Na$_2$O	wt. %	0.67	1.01	0.49	1.03	1.02	1.05	1.09	0.46	1.00	1.72 (0.46 − 3.00)
MgO	wt. %	0.60	0.70	0.57	0.55	0.78	0.58	0.78	1.08	1.24	1.43 (0.63 − 3.63)
Al$_2$O$_3$	wt. %	8.53	9.52	9.05	9.78	8.86	9.13	7.99	10.70	10.37	8.11 (5.57 − 12.1)
P$_2$O$_5$	wt. %	0.14	0.11	0.19	0.12	0.10	0.12	0.099	0.085	0.079	0.097 (0.062 − 0.14)
K$_2$O	wt. %	1.18	1.53	1.18	1.43	1.67	1.30	2.05	2.18	1.78	2.22 (1.60 − 2.81)
CaO	wt. %	11.2	5.13	5.86	6.32	0.36	12.0	0.38	0.26	0.38	0.81 (0.26 − 2.36)
TiO$_2$	wt. %	1.27	0.79	1.20	0.63	0.77	0.87	0.92	0.71	0.56	0.53 (0.32 − 0.92)
MnO	wt. %	0.26	0.22	0.18	0.19	0.073	0.21	0.070	0.081	0.11	0.12 (0.064 − 0.31)
T-Fe$_2$O$_3$	wt. %	7.85	4.41	6.21	3.76	4.20	4.12	4.22	5.85	5.71	4.52 (2.36 − 6.46)
Li	mg/kg	25	29	40	29	33	19	33	67	57	46 (19 − 76)
Be	mg/kg	1.8	1.5	1.6	1.5	1.6	1.1	1.7	2.1	2.2	2.2 (0.80 − 3.3)
Sc	mg/kg	10	9.0	11	8.1	6.8	8.2	6.9	7.4	6.4	7.4 (4.2 − 19)
V	mg/kg	107	78	114	65	78	78	88	119	111	80 (43 − 135)
Cr	mg/kg	95	52	113	59	57	39	56	74	63	54 (24 − 138)
Co	mg/kg	20	13	19	11	11	11	12	14	21	11 (5.0 − 21)
Ni	mg/kg	28	19	46	20	20	14	25	33	27	24 (12 − 39)
Cu	mg/kg	103	23	37	26	25	19	25	31	27	38 (18 − 74)
Zn	mg/kg	232	103	219	107	122	90	110	114	90	130 (90 − 198)
Ga	mg/kg	12	14	15	13	15	11	16	22	19	17 (7.0 − 23)
Rb	mg/kg	62	68	61	73	75	56	99	133	110	127 (67 − 156)
Sr	mg/kg	81	84	56	73	60	132	53	34	34	75 (33 − 125)
Y	mg/kg	26	19	30	19	11	17	10	13	13	15.1 (8.6 − 43)
Zr	mg/kg	90	80	115	85	100	74	97	77	73	67 (37 − 227)
Nb	mg/kg	14	11	12	11	12	10	14	11	8.4	8.3 (4.3 − 14)
Mo	mg/kg	1.7	1.1	1.3	0.96	0.75	0.62	0.75	1.3	0.6	1.2 (0.31 − 13)
Cd	mg/kg	4.0	1.7	6.3	1.3	0.46	0.98	0.61	0.09	0.49	0.29 (0.090 − 0.70)
Sn	mg/kg	19	5.8	7.6	3.1	4.4	2.3	4.4	3.4	2.8	3.8 (2.5 − 9.7)
Sb	mg/kg	4.7	1.8	6.0	2.1	1.4	1.1	1.4	0.97	1.6	1.2 (0.37 − 2.3)
Cs	mg/kg	6.0	8.2	11	9.3	9.3	6.6	7.7	11	13	8.9 (3.3 − 13)
Ba	mg/kg	213	366	192	283	349	295	370	450	388	401 (194 − 460)
La	mg/kg	22	19	24	21	14	17	13	22	18	19 (10 − 69)
Ce	mg/kg	41	34	41	37	29	32	25	31	28	31 (17 − 170)
Pr	mg/kg	5.2	4.5	5.8	4.9	3.5	4.1	3.3	4.7	3.7	4.4 (2.2 − 21)
Nd	mg/kg	19	16	22	17	12	15	12	18	14	17.2 (8.5 − 80)
Sm	mg/kg	3.9	3.3	4.6	3.3	2.4	2.8	2.5	3.3	2.7	3.3 (1.7 − 17)
Eu	mg/kg	0.84	0.73	1.0	0.68	0.50	0.62	0.45	0.67	0.58	0.65 (0.35 − 0.87)
Gd	mg/kg	3.6	2.9	4.0	2.8	2.0	2.5	2.0	2.9	2.5	2.9 (1.6 − 13)
Tb	mg/kg	0.53	0.47	0.62	0.42	0.31	0.38	0.31	0.49	0.41	0.49 (0.26 − 2.0)
Dy	mg/kg	3.2	2.9	3.7	2.7	1.9	2.4	1.8	2.3	2.0	2.4 (1.4 − 9.3)
Ho	mg/kg	0.60	0.54	0.69	0.51	0.35	0.45	0.34	0.43	0.40	0.47 (0.27 − 1.6)
Er	mg/kg	2.0	1.8	2.2	1.7	1.2	1.5	1.1	1.2	1.2	1.4 (0.81 − 4.8)
Tm	mg/kg	0.30	0.29	0.34	0.27	0.19	0.23	0.17	0.19	0.18	0.23 (0.12 − 0.81)
Yb	mg/kg	1.9	1.8	2.2	1.8	1.3	1.5	1.2	1.2	1.1	1.4 (0.83 − 5.3)
Lu	mg/kg	0.30	0.29	0.34	0.29	0.20	0.25	0.19	0.17	0.15	0.22 (0.12 − 0.86)
Hf	mg/kg	2.4	2.2	2.8	2.4	2.7	2.0	2.9	2.1	2.0	1.9 (1.1 − 9.8)
Ta	mg/kg	1.1	0.79	0.38	0.90	0.96	0.78	1.3	0.72	0.69	0.67 (0.39 − 1.7)
Tl	mg/kg	0.49	0.66	0.70	0.60	0.64	0.40	0.77	0.96	0.88	0.82 (0.46 − 1.0)
Pb	mg/kg	49	25	129	43	26	23	36	37	31	37 (24 − 90)
Bi	mg/kg	5.8	0.33	0.67	0.38	0.43	0.29	0.72	0.28	0.28	0.45 (0.19 − 1.4)
Th	mg/kg	8.8	7.3	7.2	8.1	7.5	5.5	9.5	7.3	5.5	7.5 (5.5 − 259)
U	mg/kg	1.8	1.6	1.4	1.5	2.2	1.6	2.6	2.8	2.4	2.2 (1.2 − 32)

[a] Two samples were also collected from Kotou River.

[b] Median (med.), minimum (min.), and maximum (max.) of elemental concentrations were calculated from the data of stream sediments derived from the accretionary complexes in Chugoku region.

Table 3.   Area of watershed and estimated ratios of exposed area of lithologies[a] distributed in each watershed.

	Watershed area	Sedimentary rock		Accretionary complex				Volcanic rock		Plutonic rock		Metamorphic rock
		Sed. A	Sed. B	Ss-Mélange	Lime-stone	Chert	Meta-basalt	Felsic	Mafic	Felsic	Mafic	
	km²	%	%	%	%	%	%	%	%	%	%	%
Akiyoshi												
No. 1	10	2.7	0	0	93	3.2	1.4	0	0	0	0	0
No. 2	78	14	28	12	30	7.6	0	0	7.5	0.9	0	0
No. 3	15	10	0	8.6	77	4.3	0	0	0	0	0	0
No. 4	16	13	24	0	52	0	0	0	10	0	0	0
No. 5	30	10	53	15	1.1	5.7	0	0	14	2.4	0	0
No. 6	131	13	17	19	35	11	0.1	0	4.5	0.5	0	0
No. 7	164	14	14	21	28	10	0.1	1.1	3.9	3.5	4.5	1.4
Imai et al. (2004)												
21006	164	14	14	21	28	10	0.1	1.1	3.9	3.5	4.5	1.4
21017	71	14	31	13	25	8.3	0	0	8.3	1.0	0	0

Sed. A: Pleistocene to Holocene sediments; Sed. B: Cretaceous sedimentary rocks; Ss-Mélange: Sandstone and melange matrix

[a] Geological Survey of Japan, AIST (ed.). 2012. Seamless digital geological map of Japan 1: 200,000. Jul 3, 2012 version. Research Information Database DB084, Geological Survey of Japan, National Institute of Advanced Industrial Science and Technology.

show the similar trends mutually. The CaO concentration is rather constant in very coarse (1–2 mm), coarse (500–1000 μm) and medium sands (250–500 μm): it increases steeply from fine sand (125–250 μm) to coarse silt (32–63 μm): becomes the highest in fine silt (<32 μm). Two samples (nos. 5 and 7) having low CaO content show the different feature: little systematic differences across grain sizes. On the other hands, variation of Sr concentration across the grain sizes is much smaller than those of CaO concentration. The Sr concentration also increases gradually with decreasing grain sizes. Adversely, Sr concentration of sample no. 1 is high in coarser grains except for very coarse sand (1–2 mm). Because Sr(II) has similar ionic radii to Ca(II), both elements are expected to have similar chemical properties mutually. However, this is not true in the study area.

Figure 4 shows the variation of concentrations of elements except for CaO and Sr against grain size of sediments. Al_2O_3 concentration of samples nos. 1, 3, and 6 is constant for all grain sizes, but that of the other samples gradually increases with decreasing grain size. The Na_2O, MgO, K_2O, Rb, and Ba concentrations are almost constant among sandy sediments, but become low in silty sediments (below 63 μm). The Sc, TiO_2, V, $T-Fe_2O_3$, and Co concentrations have the peak at fine sand (125–250 μm). For sample no. 3, the concentrations of P_2O_5, $T-Fe_2O_3$, Cr, Co, Cu, and Zn gradually decrease with decreasing the grain size. The concentrations of the other elements increase with decreasing grain size: they steeply increase below very fine sand (63–125 μm) grains (see Y in Fig. 4).

4.4 XRD patterns of stream sediments

Figure 5 shows the XRD patterns of stream sediments under 180 μm. Quartz, plagioclase and clay minerals (kaolinite and chlorite) are recognized in all samples. The high x-ray intensities were observed at 29.4°, 48.5°,

39.4°, 43.2°, and 36.0° (2θ), which are attributed to calcite. The intensities of alkali feldspar are smaller than those of plagioclase. No calcite peak is found for samples nos. 5 and 7. Accordingly, the high CaO concentration in samples nos. 1, 2, 3, 4, and 6 is explained by calcite supplied from limestone bedrocks.

Figures 6 and 7 show the XRD patterns of samples nos. 1 and 7 among various grain sizes, respectively. In sample no. 1, the peak intensities of quartz, plagioclase and K-feldspar decrease with decreasing grain size. The peak intensity of calcite increases steeply below 125 μm of grain size, which corresponds to the steep increase of CaO concentration below 125 μm of grain size (Fig. 3). Accordingly, high CaO concentration in fine grains can be explained by calcite presenting in stream sediment. The peaks of plagioclase and alkali feldspar become less prominent below the 125 μm of grain size. That change found in XRD pattern corresponds to the decrease of Na_2O and K_2O concentrations below the 125 μm of grain size (Fig. 4). The very small peak appears at 35.5° (2θ) for 63–500 μm grain size samples, which may be attributed to magnetite or pyroxene. Sample no. 7 has no peak of calcite but has intensive peaks attributed to plagioclase and alkali feldspar. The peak intensity at 27.5° of alkali feldspar becomes high in middle grain sizes (125–500μm); that at 28.0° of plagioclase becomes high in finer grains (32–125 μm). Especially, the intensive peak of alkali feldspar is notable feature for sample no. 7.

4.5 Relationship between elemental concentrations and XRD peak intensities

Yamamoto *et al*. (1998) reported that elemental concentrations of stream sediments have a good correlation to peak intensities of minerals obtained by XRD. The correlation between elemental concentrations and peak intensities of minerals were also estimated in this study. We assumed that the intensities of 12.4°, 26.6°,
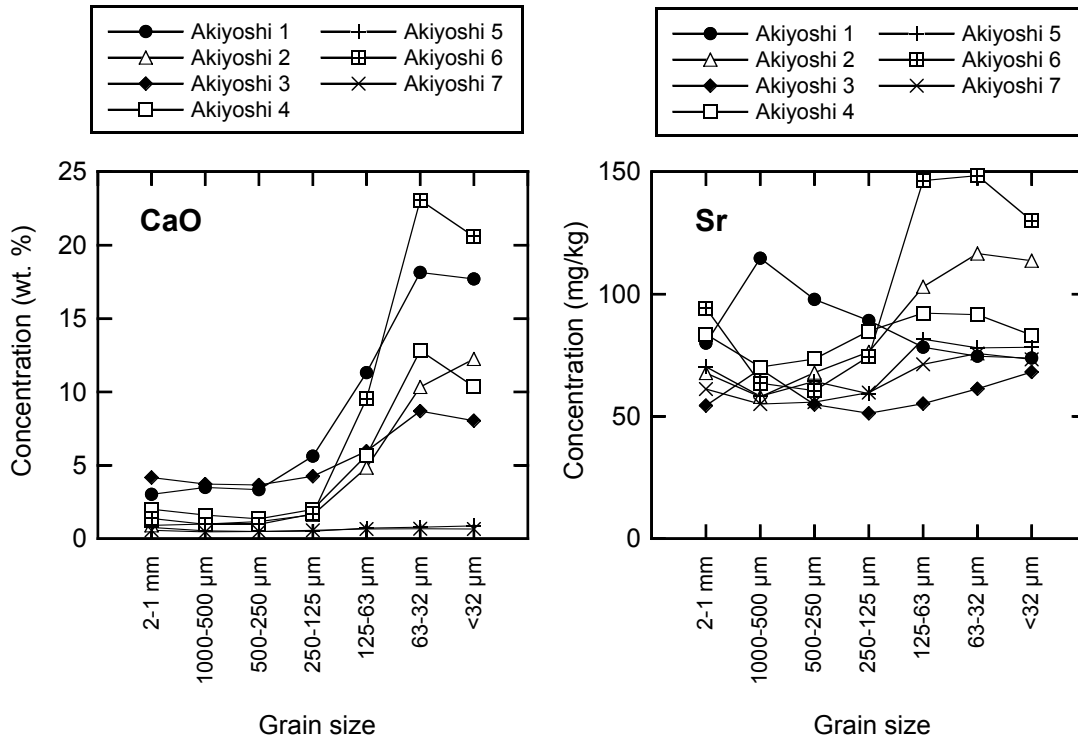
Fig 3. CaO and Sr concentrations of stream sediments according to particle size classification.

27.4°, 28.0°, and 29.4° (2θ) indicate the abundance of clay mineral, quartz, plagioclase, alkali feldspar and calcite, respectively. The peak intensities of corresponding minerals relate to their weight fractions in samples. Sample was put on a sample holder in equal amount for XRD measurement. Actually, a standard powder having object minerals (known mixing ratios) is needed for quantification of mineralogical composition (e.g., Nelson and Cochrane, 1970). Therefore, relationship between elemental concentrations and XRD peak intensities of corresponding minerals is semiquantitative evaluation.

Table 4 shows the correlation coefficients between concentrations of 12 elements and peak intensities of minerals. The peak intensity of quartz correlates negatively to P_2O_5, CaO, and MnO concentrations. The peak intensity of alkali feldspar has positive correlation with K_2O and Rb concentrations; that of plagioclase correlates to Na_2O, MgO, and Ba concentrations. The peak intensity of calcite correlates positively to CaO and Sr concentrations. The MgO, K_2O, and Rb concentrations also have positive correlation to the peak intensity of clay minerals.

Figure 8 shows the relationships between concentrations of Na_2O, K_2O, CaO, and Sr and the peak intensities of calcite, plagioclase, and alkali feldspar for all samples. There is very strong positive correlation between CaO concentration and peak intensity of calcite. On the contrary, the correlation between Sr concentration and the peak intensity of calcite is weak compared with the case of CaO. Especially, samples nos. 1 and 3 are plotted out of the positive correlation of Sr concentration and peak intensity of calcite. The Na_2O and K_2O concentrations

increase gradually with increasing the peak intensities of plagioclase and K-feldspar, respectively.

5. Discussion

5.1 Small supply of limestone clastics to river system

As we described above, the stream sediments collected in the drainage basin including Akiyoshi Limestone bedrock have high CaO concentration (5–12 wt. %). The CaO concentration is much higher than the CaO data of stream sediments derived from accretionary complexes including limestone bedrocks, which has been reported by Japanese geochemical mapping (Table 2). Thus, we confirmed the influence of limestone bedrock to river system in this study area. However, the impact on CaO abundance in stream sediments is unexpectedly small.

Watershed analysis suggests that 93% of the catchment area in the location no. 1 is occupied by limestone and that the rest is covered by Pleistocene to Holocene sediments and the chert and metabasalt of Permian accretionary complexes (Table 3). The river is an underground river for the most part, which flows through calcareous caves in Akiyoshi-dai. The river on the ground is just a few km long (around the location no. 1). Accordingly, most detritus materials would be conveyed from calcareous cave: they must consist dominantly of calcite. Because limestone has 53–55 wt. % of CaO concentration, the sample is expected to have no fewer than 50 wt. %. Actually, CaO concentration of stream sediments under 180 μm is just 12 wt. % and that of silt particle (< 63 μm) is about 18 wt. % (see Table 2 and Fig. 3). In contrast,
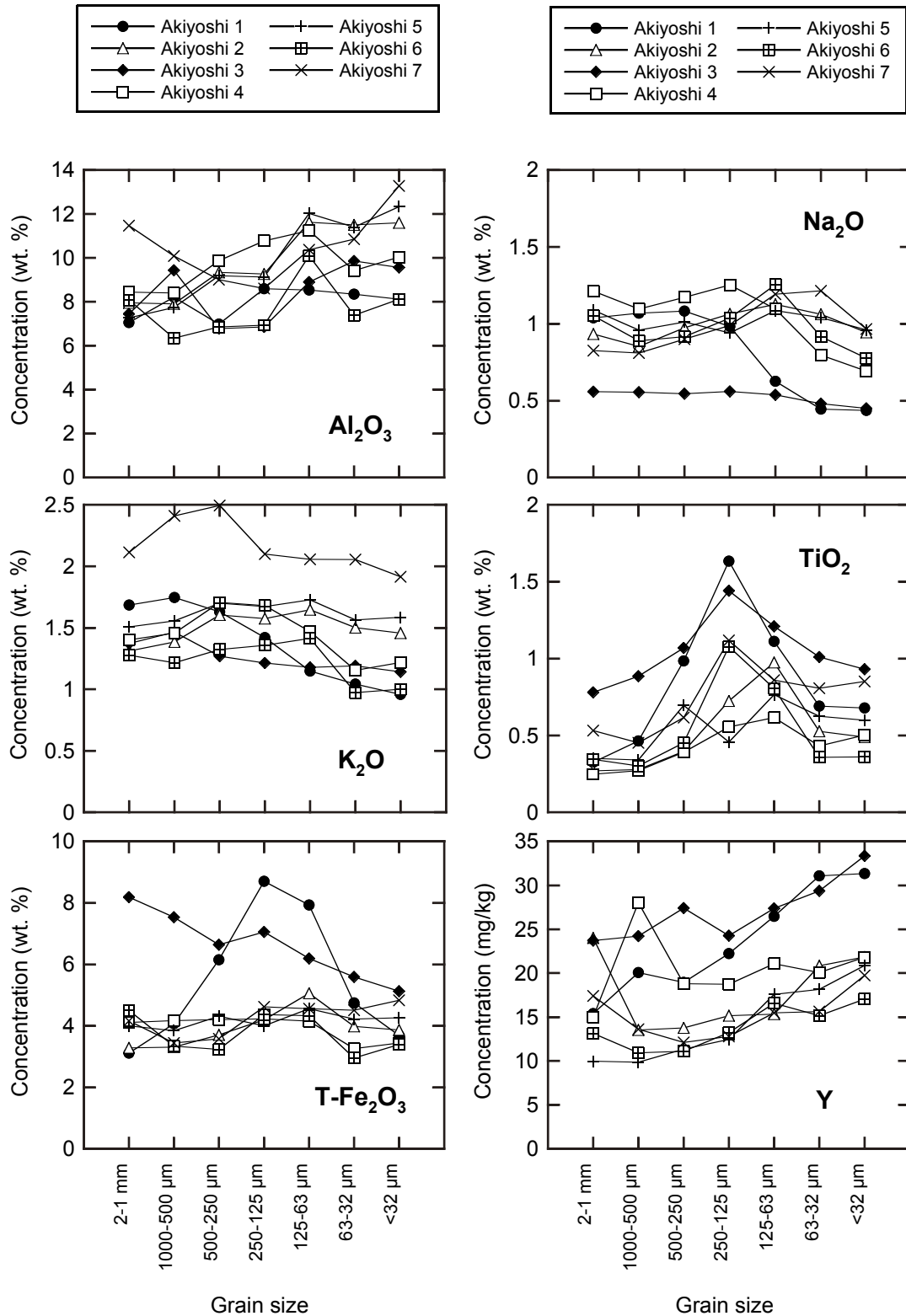
Fig 4. Elemental concentrations of stream sediments according to particle size classification.

Al_2O_3 concentrations of sample no. 1 are constant to be 7.0–8.6 wt. % irrespective to grain size (Fig. 4). In addition, the concentrations of P_2O_5 and 3d transition elements of sample no. 1 show the highest class, although these elements are not abundant in Akiyoshi Limestone (e.g., Nakano and Ishihara, 2003) (Table 2). These results suggest that particles derived from metabasalt existing narrowly are particularly significant for stream sediments

Table 4.   Correlation coefficients between elemental concentrations and peak intensities of minerals.

	Q	Pl	Kf	Cc	Cl	Na$_2$O	MgO	Al$_2$O$_3$	P$_2$O$_5$	K$_2$O	CaO	TiO$_2$	MnO	T-Fe$_2$O$_3$	Rb	Sr
Pl	0.38															
Kf	0.20	0.14														
Cc	-0.77	-0.46	-0.29													
Cl	0.11	0.44	0.51	-0.39												
Na$_2$O	0.34	0.61	0.22	-0.39	0.28											
MgO	0.14	0.66	0.25	-0.49	0.66	0.60										
Al$_2$O$_3$	-0.31	0.21	-0.09	0.00	0.37	0.24	0.47									
P$_2$O$_5$	-0.66	-0.44	-0.26	0.41	-0.14	-0.68	-0.18	0.17								
K$_2$O	0.38	0.49	0.67	-0.61	0.67	0.49	0.58	0.36	-0.39							
CaO	-0.77	-0.45	-0.31	0.99	-0.40	-0.43	-0.51	-0.04	0.42	-0.64						
TiO$_2$	-0.41	-0.10	0.20	0.12	0.12	-0.35	0.12	0.00	0.56	-0.10	0.13					
MnO	-0.72	-0.42	-0.32	0.83	-0.38	-0.29	-0.31	0.21	0.50	-0.54	0.78	0.28				
T-Fe$_2$O$_3$	-0.28	-0.15	-0.02	0.05	-0.02	-0.44	0.02	-0.11	0.64	-0.23	0.08	0.78	0.23			
Rb	0.17	0.40	0.51	-0.47	0.64	0.33	0.53	0.56	-0.23	0.91	-0.49	-0.08	-0.36	-0.21		
Sr	-0.44	0.10	-0.20	0.57	-0.14	0.39	0.08	0.21	-0.02	-0.23	0.55	-0.11	0.51	-0.17	-0.28	
Ba	0.41	0.52	0.31	-0.48	0.47	0.76	0.62	0.49	-0.63	0.74	-0.54	-0.45	-0.36	-0.58	0.68	0.10

Q: quartz, Kf: alkali feldspar, Pl: plagioclase, Cc: calcite, Cl: clay minerals

in Akiyoshi Limestone bedrocks (Fig. 1). The similar results are found in sample no. 3.

Both samples nos. 6 and 7 were collected from the main stream of Kotou River and contain wide distribution of limestone in their catchment area. Sample no. 6 has high CaO concentration but sample no. 7 has quite the low concentration. Various lithologies (granite, granodiorite, rhyolite-dacitic welded tuff, gabbro, and pelitic schist) present near the location no. 7. Sample no. 7 consists dominantly of fine sands and silt and is abundant in alkali feldspar and clay minerals (Fig. 7). The source of supply of alkali feldspar would be granite or granodiorite. The abundant clay minerals such as chlorite would be caused by weathering, which produces biotite, amphiborite, and pyroxene that are hosted in granite, granodiorite, gabbro, and politic schist. As a result, geochemistry of stream sediment is more strongly influenced by nearby lithologies in the study area. In contrast, the river basin around the location no. 6 is covered widely by sandstone and chert of Permian accretionary complexes, which are highly resistant to physical weathering. The reason why sample no. 6 has high CaO content is that the dilution effect of particles derived from those lithologies on calcite particles may be small in extent.

The Akiyoshi Limestone hardy contains any lithic fragments, because it is originated from an isolated atoll. The pure limestone is more likely to be dissolved by chemical weathering process (Fujii, 2009): the physical weathering process exercises less slight influence on limestone than chemical weathering process. Fall rains dissolve limestone bedrocks and seep into the bedrocks to form underground riverine system. Accordingly, the supply quantity of clastic materials from limestone bedrocks is much smaller than those of other rock types. In other words, most fine-sand-sized clastics of limestone may be dissolved before arriving to river system. This

is the main reason why the impact of limestone on CaO abundance in stream sediments is unexpectedly small. Most limestone bedrocks in Japan are very pure because of isolated atoll-origin as with the case of the Akiyoshi. The less influence of limestone on geochemical maps would be explained by the same reason. Incidentally, it is unlikely that calcite clastics in stream sediments are totally dissolved between locations nos. 6 and no. 7 because the total stream length between two points is just 13 km. If calcite clastics were dissolved in such short distances, significant loss of CaO in stream sediments would be also found between sampling locations nos. 6 and 1 (or nos. 2 and 3).

5.2 Influence of calcite formed secondarily

Figures 3 and 5 reveal that calcite debris supplied from host rocks to river system is abundant in finer particles. However, it is expected that finer calcite particle is dissolved in stream water faster than coarser calcite because fine particle has a larger surface area than coarse grain. Finer calcite particles may be supplied through limestone mine activity. However, digging area of limestone is found only in the watershed of sample no. 3. Accordingly we assumed that calcite is formed secondarily in limestone cave or in river system to which groundwater flowing through limestone bedrock is supplied because calcium carbonate is oversaturated by CO_2 degassing process (e.g., Kashima, 2010). Calcite aggregated may cover fine clastic materials and clay minerals. Calcite formed secondarily can explain the different behavior of Sr from CaO in sample no. 1 (also no. 3). The origin of ground water in Akiyoshi-dai is meteoric water. The Sr concentration in ground water possibly changes largely based on the rainfall level. As a result, Sr concentration of calcite formed secondarily changes largely from that in limestone. The Sr concentration does not have good positive correlation
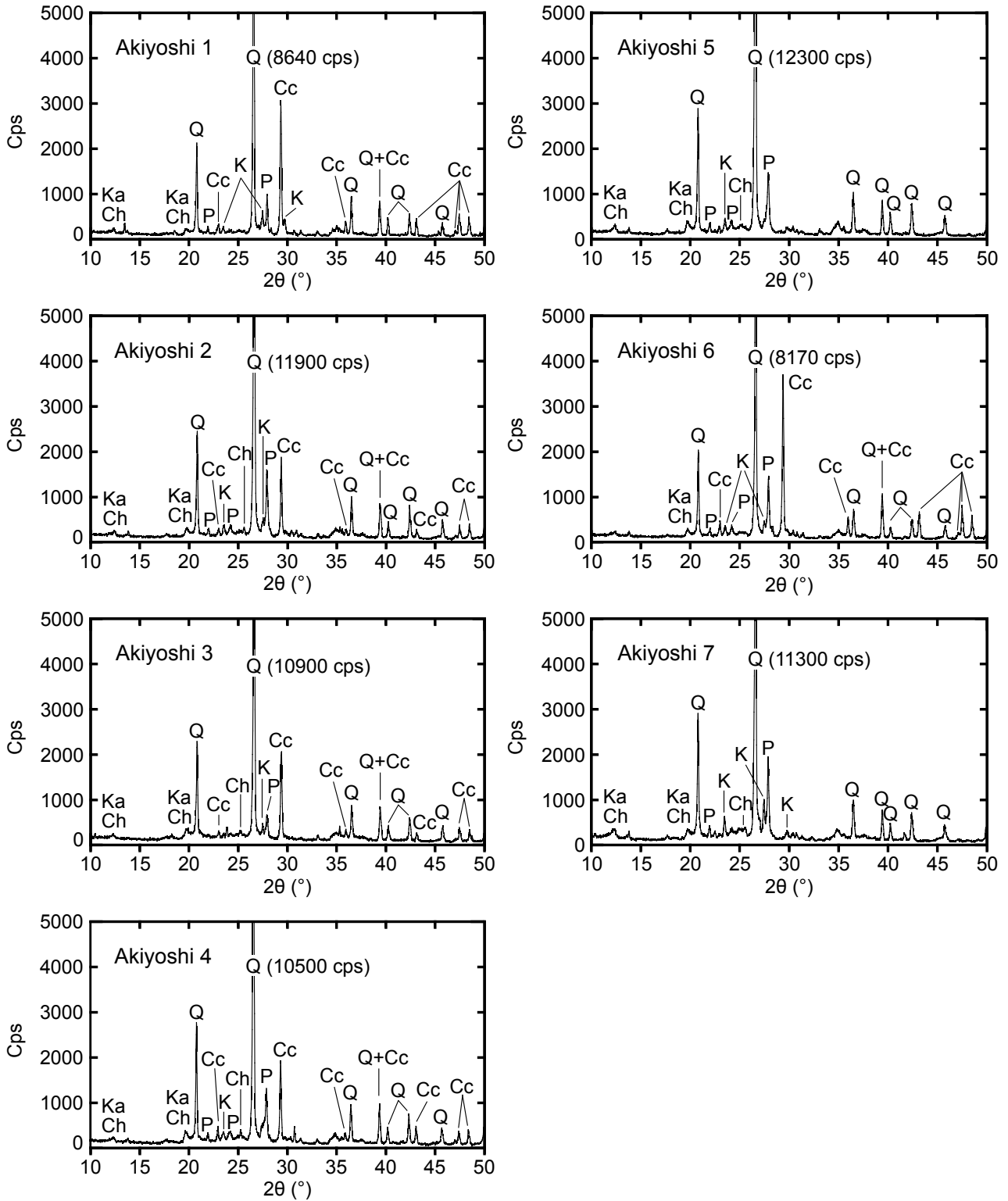
Fig 5. XRD patterns of stream sediments sieved with a 180 μm screen. Abbreviation Q, P, K, Cc, Ka, and Ch indicate quartz, plagioclase, alkali feldspar, calcite, kaolinite and chlorite, respectively.

to CaO concentration because stream sediments derived from limestone bedrock area are composed of the mixture of limestone clastics, calcite formed secondarily, and clastics except for limestone. The hypothesis proposed here will be validated in the following paper using Sr isotope ratio of stream sediments in this study area.
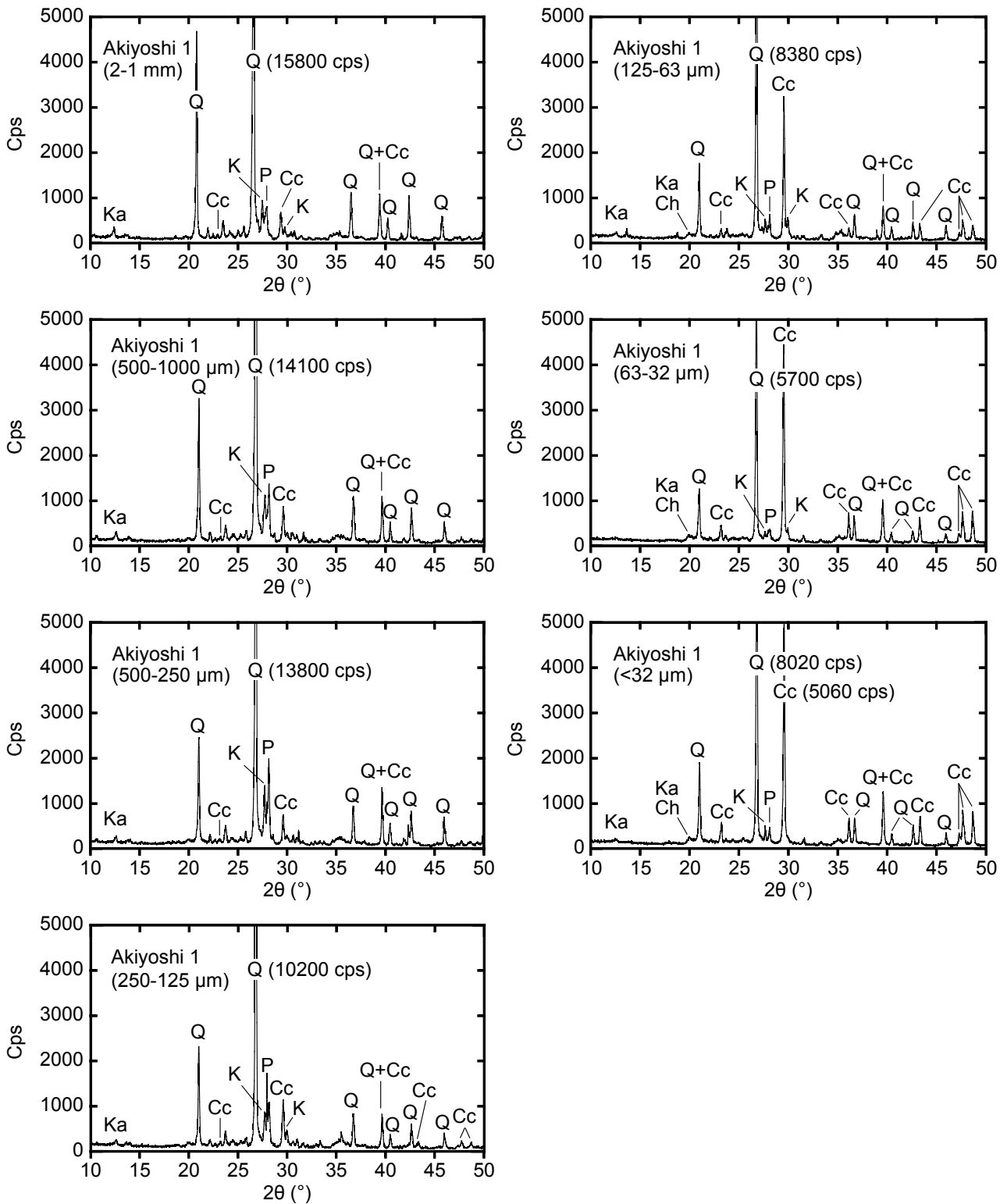
Fig 6. XRD patterns of stream sediment (sample no. 1) grouped into 7 grain sizes. Abbreviation Q, P, K, Cc, Ka, and
Ch are the same as Fig. 4.
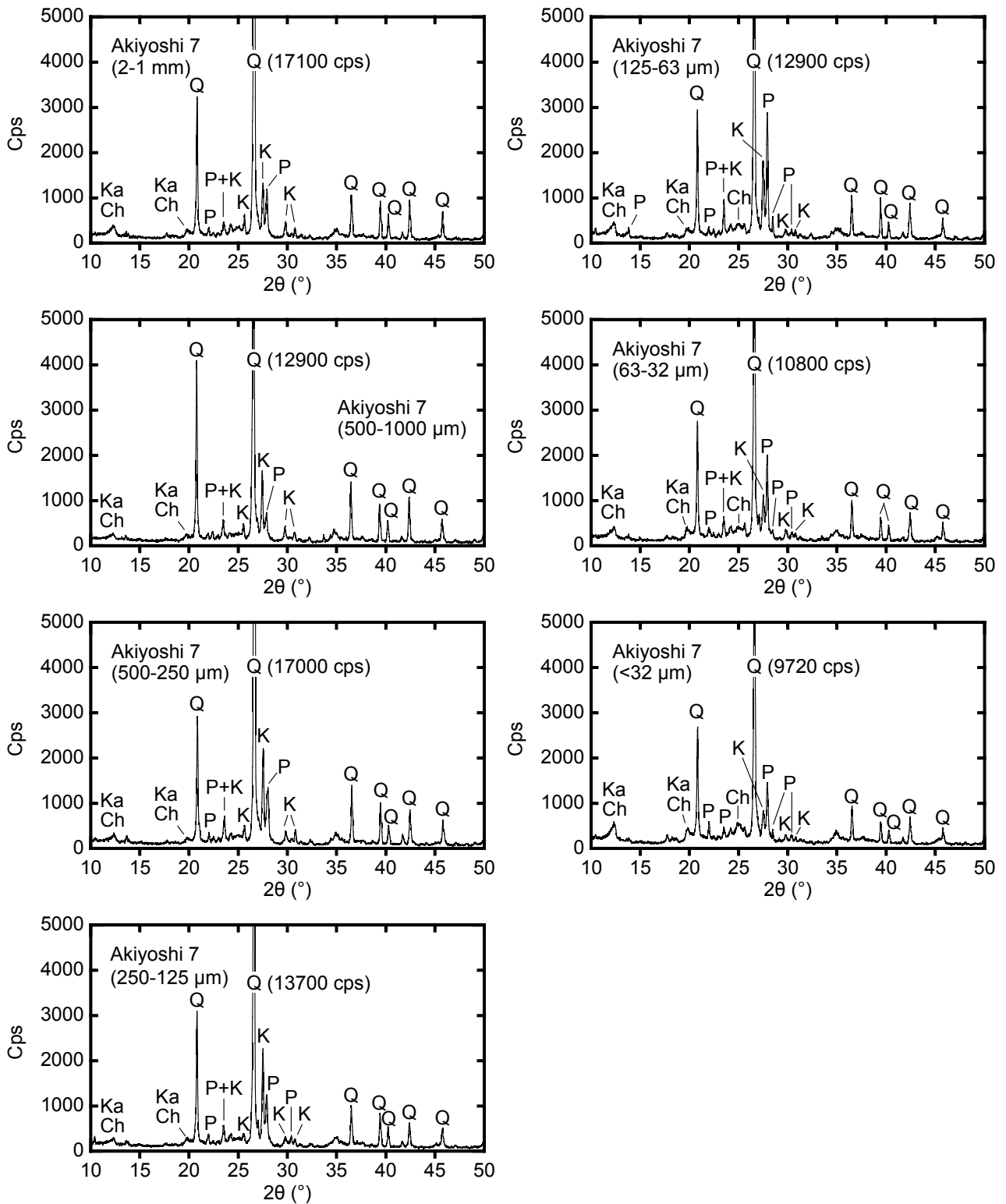
Fig 7. XRD patterns of stream sediment (sample no. 7) grouped into 7 grain sizes. Abbreviation Q, P, K, Cc, Ka, and Ch are the same as Fig. 4.
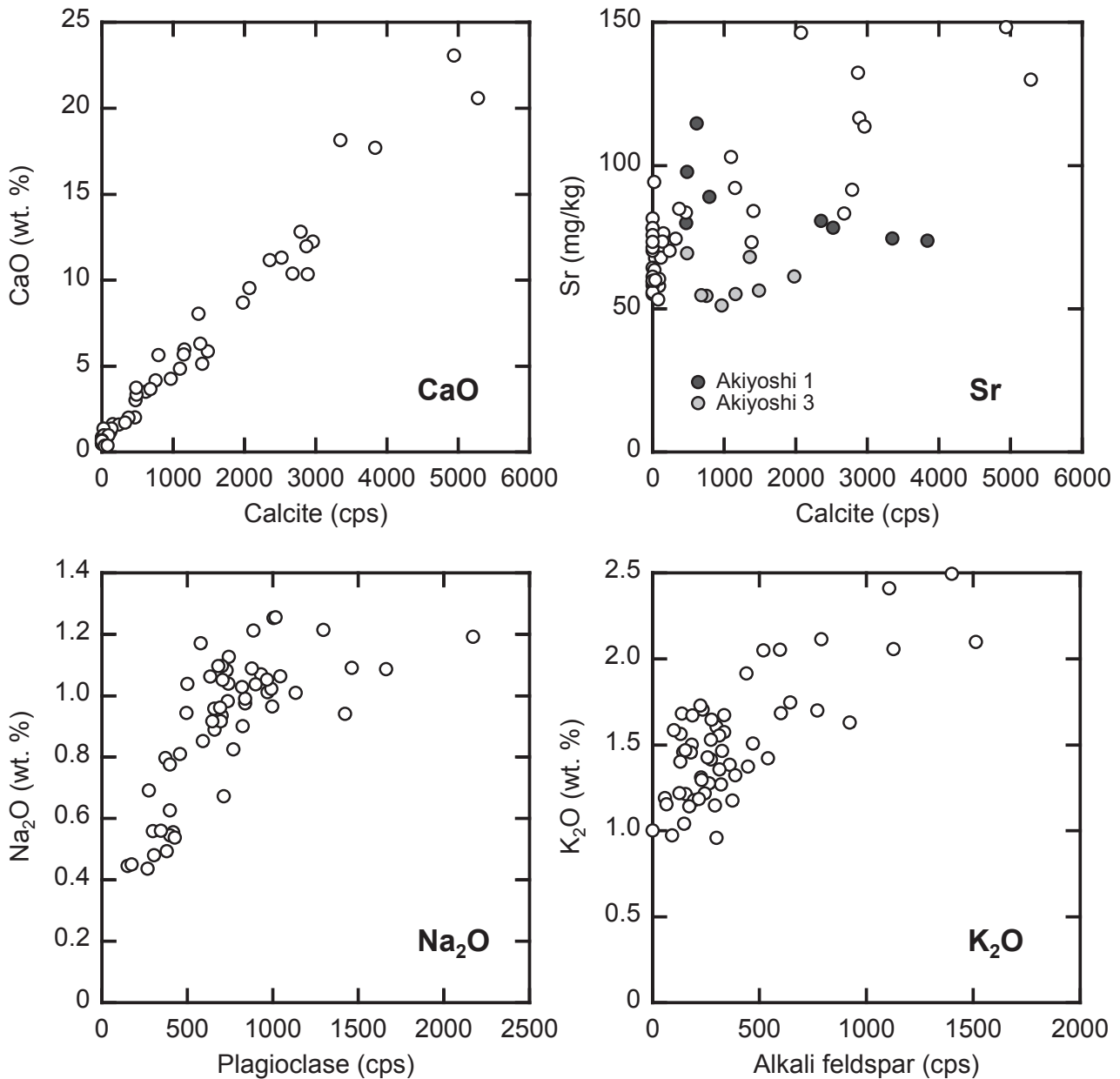
Fig 8. Relationships between elemental concentrations and peak intensities of minerals obtained by XRD. The intensities of the peaks at 27.4°, 28.0° and 29.4° (2θ) are assigned as plagioclase, alkali feldspar and calcite, respectively.

6. Summary

We elucidated why the impact of limestone to nationwide CaO and Sr maps in Japan is obscured. Seven stream sediment samples were collected from the Akiyoshi-dai that is underlain by the largest limestone bedrock in Japan. The 51 elemental concentrations and mineralogical compositions were determined for these samples. Stream sediments derived from the Akiyoshi-dai area have the high CaO concentration and the intensive peak of calcite in the XRD pattern. However the contribution is restricted to a small area. High concentrations of elements except for CaO

and Sr such as Al_2O_3 (8.5–9.0 wt. %) and T-Fe_2O_3 (6.2–7.9 wt. %) are found even in samples whose drainage basins dominantly expose limestone. Eventually, it is concluded that small amount of limestone clastics is supplied to river system because pure limestone originated from an isolated atoll is more likely to be subjected to chemical weathering process more than physical weathering and erosion processes. Geochemical maps have been created on the assumption that stream sediment is a composite sample of the materials distributing in the catchment area: its geochemistry is controlled conclusively by parent lithology. We have assumed that the influence of parent

lithology on elemental abundance of stream sediments correlates simply to its exposed area in each watershed of samples. The rule is inapplicable to limestone.

References

Albanese, S., De Vivo, B., Lima, A. and Cicchella, D. (2007) Geochemical background and baseline values of toxic elements in stream sediments of Campania region (Italy). *J. Geochem. Explor*. **93**, 21-34.

De Vos, W., Tarvainen, T., Salminen, R., Reeder, S., De Vivo, B., Demetriades, A., Pirc, S., Batista, M. J., Marsina, K., Ottesen, R.-T., O'Connor, P. J., Bidovec, M., Lima, A., Siewers, U., Smith, B., Taylor, H., Shaw, R., Salpeteur, I., Gregorauskiene, V., Halamic, J., Slaninka, I., Lax, K., Gravesen, P., Birke, M., Breward, N., Ander, E. L., Jordan, G., Duris, M., Klein, P., Locutura, J., Bel-lan, A., Pasieczna, A., Lis, J., Mazreku, A., Gilucis, A., Heitzmann, P., Klaver, G. and Petersell, V. (2006) *Geochemical atlas of Europe. Part 2 - Interpretation of Geochemical Maps, Additional Tables, Figures, Maps, and Related Publications*. Geological Survey of Finland, Espoo, Finland, 692 pp.

Fujii, A. (2009) A Report on the Public Symposium "Mammal fossils in the Cenozoic Era preserved in limestone caves of the Akiyoshi-dai Plateau" at the Annual Meeting of the Mammalogical Society of Japan (2008): Caves of the Akiyoshi-dai Plateau and their chronology based on the rate of downward erosion of the Koto-gawa River. *Honyurui Kagaku (Mammalian Science)* **49**, 91-95 (in Japanese).

Geological Survey of Japan, AIST (2012) Seamless digital geological map of Japan 1: 200,000. Jul 3, 2012 version. (Geological Survey of Japan, A., ed.). *Research Information Database DB084, Geological Survey of Japan, National Institute of Advanced Industrial Science and Technology*. Geological Survey of Japan, AIST, Tsukuba.

Howarth, R. J. and Thornton, I. (1983) Regional Geochemical Mapping and its Application to Environmental Studies. Applied *Environmental Geochemistry*. (Thornton, I., ed.), 41-73, Academic Press London.

Imai, N., Terashima, S., Ohta, A., Mikoshiba, M., Okai, T., Tachibana, Y., Togashi, S., Matsuhisa, Y., Kanai, Y. and Kamioka, H. (2004) *Geochemical map of Japan*. Geological Survey of Japan, AIST, 209 pp (in Japanese with English astract).

Kashima, N. (2010) Speleominerals and *Cave Environment. Cave Environmental NET Society (CENS)* **1**, 3-6 (in Japanese with English astract).

Matsuura, H., Ozaki, M., Wakita, K., Makimoto, H., Mizuno, K., Kametaka, M., Sudo, S., Morijiri, R. and Komazawa, M. (2007) Yamagushi and Mishima. *Geological Map of Japan 1:200,000*. Geological Survey of Japan, AIST, Tsukuba.

Nakano, T. and Ishihara, S. (2003) Geochemical characteristics of the Akiyoshi limestones, Japan and their bearing on exploration for blind skarn deposits. *Resour. Geol*. **53**, 29-36.

Nelson, C. S. and Cochran, R.H.A. (1970) A rapid x-ray method for the quantitative determination of selected minerals in fine-grained and altered rocks. *Tane* **16**, 151-162.

Ohta, A., Imai, N., Terashima, S. and Tachibana, Y. (2004a) Investigation of elemental behaviors in Chugoku region of Japan based on geochemical map utilizing stream sediments. *Chikyukagaku (Geochemistry)* **38**, 203-222 (in Japanese with English astract).

Ohta, A., Imai, N., Terashima, S. and Tachibana, Y. (2005) Application of multi-element statistical analysis for regional geochemical mapping in Central Japan. *Appl. Geochem*. **20**, 1017-1037.

Ohta, A., Imai, N., Terashima, S., Tachibana, Y., Ikehara, K. and Nakajima, T. (2004b) Geochemical mapping in Hokuriku, Japan: influence of surface geology, mineral occurrences and mass movement from terrestrial to marine environments. *Appl. Geochem*. **19**, 1453-1469.

Sano, H. and Kanmera, K. (1991) Collapse of ancient oceanic reef complex -What happened during collision of Akiyoshi reef complex?- Sequence of collisional collapse and generation of collapse products. *Journal of Geological Society of Japan* **97**, 631-644.

Yamamoto, K., Tanaka, T., Kawabe, I., Iwamori, H., Hirahara, Y., Asahara, Y., Kim, K. H., Richardson, C., Ito, T., Dragusanu, C., Miura, N., Aoki, H., Ohta, A., Sakakibara, T., Tanimizu, M., Mizutani, Y., Miyanaga, N., Murayama, M., Senda, R., Takayanagi, Y., Inoue, Y., Kawasaki, K., Takagi, M., Kawasaki, K., Nebu, S. and Inayoshi, M. (1998) Geochemical map of the Ryoke granitic area in the northeastern part of Toyota City, Aichi Prefecture. *Jour. Geol. Soc. Japan* **104**, 688-704 (in Japanese with English astract).

Appendix Table. Elemental concentrations of stream sediments groupded into 7 grain sizes.

		Akiyoshi 1							Akiyoshi 2							Akiyoshi 3							Akiyoshi 4						
		A	B	C	D	E	F	G	A	B	C	D	E	F	G	A	B	C	D	E	F	G	A	B	C	D	E	F	G
Na_2O	wt. %	1.04	1.07	1.08	0.98	0.63	0.45	0.44	0.93	0.85	0.98	1.06	1.13	1.06	0.94	0.56	0.56	0.55	0.56	0.54	0.48	0.45	1.21	1.10	1.17	1.25	1.10	0.80	0.69
MgO	wt. %	0.63	0.71	0.85	0.86	0.55	0.39	0.35	0.56	0.57	0.64	0.70	0.83	0.76	0.73	0.64	0.60	0.57	0.61	0.52	0.57	0.49	0.57	0.57	0.64	0.68	0.66	0.57	0.59
Al_2O_3	wt. %	7.05	8.22	6.99	8.60	8.54	8.35	8.13	7.96	7.91	9.35	9.27	11.6	11.5	11.6	7.45	9.44	6.78	6.86	8.90	9.86	9.57	8.44	8.41	9.88	10.8	11.2	9.43	10.0
P_2O_5	wt. %	0.079	0.091	0.11	0.13	0.14	0.13	0.12	0.070	0.069	0.079	0.082	0.12	0.14	0.15	0.23	0.21	0.17	0.18	0.19	0.21	0.20	0.073	0.076	0.085	0.092	0.13	0.13	0.15
K_2O	wt. %	1.68	1.75	1.63	1.42	1.15	1.04	0.96	1.31	1.38	1.61	1.58	1.65	1.50	1.46	1.37	1.47	1.27	1.21	1.18	1.19	1.14	1.40	1.46	1.71	1.68	1.47	1.16	1.22
CaO	wt. %	3.03	3.50	3.34	5.64	11.3	18.1	17.7	0.92	1.01	1.17	1.63	4.85	10.3	12.2	4.17	3.74	3.67	4.26	5.97	8.70	8.04	2.02	1.61	1.37	2.00	5.69	12.8	10.4
TiO_2	wt. %	0.32	0.46	0.98	1.63	1.11	0.69	0.68	0.27	0.28	0.40	0.72	0.97	0.53	0.49	0.78	0.88	1.07	1.44	1.21	1.01	0.93	0.25	0.27	0.39	0.56	0.62	0.43	0.50
MnO	wt. %	0.063	0.091	0.13	0.22	0.28	0.20	0.19	0.089	0.077	0.10	0.14	0.24	0.29	0.36	0.12	0.12	0.12	0.16	0.18	0.19	0.18	0.12	0.099	0.096	0.13	0.21	0.25	0.34
$T\text{-}Fe_2O_3$	wt. %	3.12	4.07	6.15	8.70	7.94	4.75	3.69	3.29	3.31	3.71	4.19	5.06	3.98	3.87	8.18	7.54	6.64	7.06	6.19	5.59	5.13	4.11	4.17	4.21	4.23	4.15	3.26	3.45
Li	mg/kg	25	28	30	49	35	34	32	35	35	40	41	46	41	43	51	49	47	55	56	57	55	34	35	41	41	42	37	40
Be	mg/kg	1.1	1.3	1.5	1.7	1.8	1.6	1.5	1.3	1.3	1.3	1.4	1.5	1.5	1.6	1.5	1.4	1.4	1.5	1.5	1.6	1.4	1.4	1.4	1.5	1.6	1.6	1.4	1.5
Sc	mg/kg	7.0	8.7	9.2	11.9	9.8	8.4	8.3	5.9	5.8	6.6	8.0	10	9.8	9.6	10	11	9.9	11	11	12	11	5.7	6.0	6.4	7.5	8.7	7.3	8.2
V	mg/kg	51	58	93	134	98	68	60	45	46	56	73	92	67	61	112	111	116	136	115	101	87	44	50	56	62	66	51	55
Cr	mg/kg	39	57	71	82	122	105	99	37	40	49	47	60	51	54	134	135	113	117	110	133	131	42	50	49	50	58	55	63
Co	mg/kg	11	13	17	20	21	18	17	7.6	8.8	11	11	13	19	14	22	19	17	20	18	17	16	8.1	8.7	10	10	11	11	12
Ni	mg/kg	14	17	19	23	27	27	35	14	14	15	16	20	19	23	46	44	39	43	43	50	51	13	13	16	18	20	19	24
Cu	mg/kg	27	38	41	50	76	88	87	18	17	19	19	26	28	28	35	34	31	38	40	41	38	24	20	20	24	32	35	41
Zn	mg/kg	78	113	172	220	236	217	202	52	59	77	85	110	101	101	183	181	185	226	221	206	183	89	77	88	95	105	92	105
Ga	mg/kg	10	11	12	13	12	11	11	10	10	12	13	15	14	14	14	14	13	15	14	14	13	11	12	13	14	14	12	13
Rb	mg/kg	70	73	69	68	61	59	58	64	67	78	75	80	78	78	64	70	63	61	54	67	68	71	74	88	86	88	72	79
Sr	mg/kg	80	115	98	89	78	75	74	68	58	68	76	103	117	114	55	69	55	51	55	61	68	84	70	73	85	92	92	83
Y	mg/kg	15	20	19	22	26	31	31	24	14	14	15	15	21	22	24	24	27	24	27	29	33	15	28	19	19	21	20	22
Zr	mg/kg	59	60	64	76	98	107	102	66	65	70	73	94	88	90	98	100	95	109	125	124	129	61	64	73	78	94	84	95
Nb	mg/kg	4.8	6.3	7.7	15	14	12	12	5.4	5.6	6.8	9.8	13	8.4	8.1	10	11	9.8	9.5	12	13	14	5.6	6.3	7.7	9.9	11	8.3	10
Mo	mg/kg	0.47	0.60	0.69	1.1	0.95	1.2	1.7	0.35	0.38	0.41	0.49	0.83	0.64	0.77	1.4	1.2	1.3	1.2	1.1	1.2	1.6	0.56	0.55	0.47	0.50	0.82	0.63	0.84
Cd	mg/kg	1.0	1.5	2.0	2.7	4.0	5.4	5.8	0.65	0.61	0.80	1.1	1.8	2.1	2.6	2.9	3.4	4.0	5.7	6.4	6.8	5.6	0.57	0.51	0.64	0.84	1.4	1.6	2.0
Sn	mg/kg	2.9	8.1	11	20	12	14	14	1.8	2.0	2.2	3.1	3.0	3.3	4.6	5.1	5.3	6.6	6.3	9.7	7.9	9.4	2.1	2.6	2.6	3.1	3.7	3.1	5.3
Sb	mg/kg	1.5	2.4	2.7	3.4	5.5	5.3	4.3	1.6	1.3	1.5	1.6	2.0	1.6	1.6	6.0	5.8	4.6	5.1	5.9	5.9	5.4	3.6	2.2	2.0	2.1	1.9	1.6	1.7
Cs	mg/kg	3.4	4.1	4.3	5.2	6.3	6.7	6.6	5.6	5.8	7.1	7.3	9.6	9.8	10	8.5	9.1	8.4	10	11	11	11	5.4	6.1	7.9	9.0	10	9.3	10
Ba	mg/kg	316	343	289	238	209	201	212	371	350	375	362	401	392	403	209	222	202	202	194	197	211	351	334	356	342	308	255	287
La	mg/kg	14	15	14	19	23	25	30	38	15	14	14	15	24	23	34	17	19	17	19	24	29	16	17	14	16	21	22	26
Ce	mg/kg	27	28	25	35	44	47	57	66	25	25	25	26	44	43	68	31	37	28	31	39	43	27	30	26	31	41	44	53
Pr	mg/kg	3.4	3.7	3.7	4.5	5.3	5.9	7.1	7.3	3.4	3.2	3.2	3.4	5.4	5.3	8.8	4.2	4.7	4.1	4.7	5.8	6.9	3.4	3.6	3.2	3.7	4.7	5.0	6.0
Nd	mg/kg	12	14	14	16	19	21	25	26	12	11	12	12	19	19	32	16	18	16	18	21	26	12	13	12	13	17	18	21
Sm	mg/kg	2.6	3.1	2.9	3.4	3.9	4.3	4.9	2.4	2.3	2.3	2.4	3.7	3.8	4.1	3.5	3.8	3.3	3.7	4.3	5.0	5.3	2.3	2.6	2.3	2.5	3.3	3.4	4.0
Eu	mg/kg	0.57	0.76	0.70	0.76	0.83	0.92	1.0	0.51	0.48	0.51	0.57	0.77	0.84	0.88	0.87	0.96	0.84	0.90	1.0	1.1	1.2	0.50	0.53	0.48	0.57	0.68	0.70	0.77
Gd	mg/kg	2.5	2.9	2.8	3.1	3.6	3.9	4.3	2.2	2.0	2.2	2.3	3.2	3.4	3.7	3.4	3.7	3.2	3.5	4.0	4.6	4.8	2.2	2.6	2.1	2.2	2.8	3.0	3.5
Tb	mg/kg	0.37	0.45	0.43	0.48	0.54	0.59	0.62	0.33	0.32	0.35	0.35	0.50	0.52	0.55	0.53	0.58	0.50	0.55	0.59	0.68	0.68	0.34	0.49	0.38	0.39	0.46	0.44	0.50
Dy	mg/kg	2.2	2.8	2.6	2.8	3.2	3.6	3.7	2.0	2.0	2.2	2.3	3.0	3.1	3.3	3.1	3.4	3.0	3.3	3.6	4.0	4.0	2.1	3.6	2.6	2.5	2.8	2.6	2.9
Ho	mg/kg	0.40	0.51	0.49	0.54	0.62	0.69	0.68	0.38	0.39	0.44	0.45	0.58	0.58	0.60	0.58	0.64	0.56	0.61	0.67	0.74	0.73	0.43	0.84	0.54	0.51	0.53	0.48	0.53
Er	mg/kg	1.3	1.6	1.5	1.7	1.9	2.2	2.1	1.3	1.3	1.5	1.5	1.8	1.8	1.9	1.9	2.1	1.8	2.1	2.1	2.4	2.4	1.4	3.0	1.8	1.7	1.7	1.6	1.7
Tm	mg/kg	0.20	0.25	0.24	0.27	0.31	0.34	0.34	0.19	0.21	0.24	0.25	0.29	0.29	0.30	0.29	0.31	0.28	0.30	0.33	0.37	0.36	0.23	0.50	0.30	0.29	0.28	0.24	0.27
Yb	mg/kg	1.3	1.6	1.5	1.7	1.9	2.1	2.1	1.3	1.4	1.6	1.6	1.9	1.9	1.9	1.8	1.9	1.8	1.9	2.1	2.3	2.3	1.6	3.4	2.0	1.9	1.8	1.6	1.7
Lu	mg/kg	0.21	0.25	0.25	0.27	0.31	0.33	0.33	0.21	0.23	0.26	0.26	0.30	0.29	0.30	0.30	0.32	0.29	0.32	0.36	0.37	0.36	0.25	0.55	0.32	0.31	0.30	0.25	0.28
Hf	mg/kg	1.6	1.7	1.8	2.1	2.8	3.0	2.7	1.8	1.8	2.0	2.0	2.7	2.5	2.5	2.5	2.4	2.3	2.7	3.1	3.1	3.3	1.8	1.9	2.1	2.2	2.6	2.3	2.5
Ta	mg/kg	0.36	0.38	0.24	0.99	1.1	0.94	1.1	0.51	0.52	0.60	0.70	0.87	0.79	0.76	0.40	0.65	0.17	0.18	0.32	0.94	1.1	0.52	0.59	0.71	0.86	0.97	0.77	0.94
Tl	mg/kg	0.44	0.49	0.52	0.52	0.49	0.49	0.48	0.52	0.53	0.61	0.62	0.69	0.67	0.67	0.61	0.64	0.61	0.69	0.70	0.71	0.67	0.51	0.51	0.62	0.63	0.63	0.54	0.60
Pb	mg/kg	87	32	33	43	52	55	61	13	15	18	21	32	25	30	136	128	114	124	131	128	107	28	30	30	31	36	37	44
Bi	mg/kg	0.90	2.1	2.9	6.0	8.8	5.6	4.8	0.25	0.21	0.23	0.27	0.36	0.34	0.36	0.46	0.49	0.49	0.66	0.77	0.66	0.57	0.26	0.28	0.25	0.29	0.39	0.35	0.40
Th	mg/kg	5.8	5.7	5.9	8.0	8.8	8.0	8.9	6.2	6.3	6.9	6.7	9.2	8.0	8.3	5.4	6.2	5.5	6.0	7.0	8.7	8.4	6.8	6.6	7.5	7.8	8.6	8.0	8.9
U	mg/kg	1.3	1.4	1.2	1.7	1.9	2.0	1.8	1.6	1.6	1.7	1.8	2.1	1.9	1.8	1.4	1.4	1.3	1.5	1.4	1.5	1.9	1.8	1.8	1.8	1.9	2.1	1.7	1.8

A: 1-2mm, B: 500–1000 μm, C: 250–500 μm, D: 125–250 μm, E: 63–125 μm, F: 32–63 μm, G: <32 μm

Appendix Table. continued.

		Akiyoshi 5							Akiyoshi 6							Akiyoshi 7						
		A	B	C	D	E	F	G	A	B	C	D	E	F	G	A	B	C	D	E	F	G
Na_2O	wt. %	1.09	0.96	1.01	0.94	1.09	1.04	0.96	1.05	0.89	0.92	1.04	1.26	0.92	0.78	0.83	0.81	0.90	0.99	1.19	1.21	0.97
MgO	wt. %	0.85	0.78	0.87	0.81	0.93	0.88	0.92	0.68	0.55	0.56	0.67	0.73	0.55	0.61	0.68	0.59	0.66	0.79	0.92	1.01	1.04
Al_2O_3	wt. %	7.27	7.75	9.18	9.14	12.0	11.4	12.3	8.09	6.35	6.86	6.94	10.1	7.39	8.13	11.5	10.1	9.01	8.61	10.4	10.9	13.3
P_2O_5	wt. %	0.085	0.077	0.086	0.080	0.11	0.13	0.15	0.089	0.065	0.064	0.074	0.12	0.12	0.18	0.11	0.087	0.080	0.096	0.10	0.11	0.12
K_2O	wt. %	1.51	1.56	1.70	1.67	1.73	1.56	1.59	1.28	1.22	1.32	1.36	1.42	0.97	1.00	2.11	2.41	2.49	2.10	2.06	2.05	1.92
CaO	wt. %	0.77	0.54	0.51	0.52	0.73	0.80	0.88	1.38	0.99	0.98	1.71	9.55	23.1	20.6	0.58	0.47	0.49	0.58	0.67	0.70	0.66
TiO_2	wt. %	0.35	0.34	0.70	0.46	0.76	0.63	0.60	0.34	0.30	0.45	1.08	0.81	0.36	0.36	0.53	0.45	0.62	1.12	0.86	0.81	0.85
MnO	wt. %	0.060	0.054	0.065	0.057	0.083	0.087	0.11	0.068	0.056	0.071	0.11	0.20	0.22	0.29	0.079	0.059	0.059	0.082	0.075	0.071	0.076
$T\text{-}Fe_2O_3$	wt. %	4.00	3.84	4.31	4.00	4.56	4.22	4.27	4.50	3.34	3.23	4.36	4.33	2.95	3.40	4.17	3.45	3.58	4.62	4.56	4.51	4.83
Li	mg/kg	39	38	45	42	48	48	50	31	30	32	31	30	21	24	39	33	33	37	48	48	56
Be	mg/kg	1.3	1.3	1.4	1.4	1.6	1.6	1.7	1.2	1.0	1.1	1.1	1.2	0.9	1.0	1.6	1.4	1.4	1.6	1.7	1.8	2.0
Sc	mg/kg	5.6	5.2	6.8	6.0	10	9.3	10	6.7	5.1	5.4	7.1	8.6	6.0	6.9	8.2	6.3	5.7	7.1	8.1	9.1	12
V	mg/kg	56	54	74	63	78	75	69	64	48	49	80	75	47	52	68	57	62	96	85	85	89
Cr	mg/kg	36	37	54	43	54	59	60	28	30	30	46	47	32	35	43	36	36	49	53	57	64
Co	mg/kg	9.6	9.8	10	10	11	11	12	9.5	8.6	8.8	10	12	8.2	10	11	8.9	9.1	11	12	12	13
Ni	mg/kg	17	15	18	16	21	22	26	14	13	12	13	16	7.9	13	20	17	18	20	24	26	31
Cu	mg/kg	22	22	26	23	32	39	43	19	16	16	18	28	23	28	30	25	26	31	36	40	46
Zn	mg/kg	82	96	113	109	121	124	135	59	56	63	80	98	74	88	87	74	68	95	105	110	125
Ga	mg/kg	12	12	14	13	16	15	16	11	9.3	9.8	11	12	8.7	10	15	13	13	14	17	17	20
Rb	mg/kg	70	75	85	83	87	83	91	57	52	57	57	60	43	48	113	126	128	108	108	111	112
Sr	mg/kg	70	58	64	59	82	78	78	94	64	61	74	146	148	130	61	55	56	60	71	76	73
Y	mg/kg	10	9.9	11	12	18	18	21	13	11	11	13	17	15	17	17	14	12	13	16	16	20
Zr	mg/kg	71	74	89	81	101	108	105	69	63	71	75	86	67	60	88	62	66	80	106	135	145
Nb	mg/kg	6.1	6.3	11	7.6	12	11	11	5.4	4.8	6.2	11	10	4.8	5.0	8.8	7.9	10	16	13	13	14
Mo	mg/kg	0.41	0.42	0.60	0.46	0.62	0.64	1.1	0.48	0.38	0.36	0.50	0.74	0.47	0.65	0.59	0.70	0.59	0.80	0.65	0.59	0.64
Cd	mg/kg	0.23	0.25	0.40	0.32	0.53	0.61	0.76	0.27	0.30	0.42	0.57	1.0	1.2	1.5	0.46	0.42	0.41	0.58	0.67	0.68	0.76
Sn	mg/kg	2.3	2.6	3.8	6.7	3.6	4.7	6.1	1.5	1.5	1.7	2.2	2.7	1.7	2.9	3.4	2.8	3.2	4.6	4.6	4.6	5.5
Sb	mg/kg	1.7	1.5	1.2	1.4	1.4	1.4	1.4	1.2	0.99	1.0	1.1	1.3	0.91	1.1	1.2	1.0	1.0	1.1	1.3	1.4	1.4
Cs	mg/kg	6.0	6.5	9.0	8.1	11	11	12	5.0	4.5	5.1	5.3	7.4	5.6	6.6	8.1	7.1	7.0	7.4	8.3	8.7	9.7
Ba	mg/kg	338	334	347	342	365	351	388	304	285	297	305	326	237	257	384	394	394	362	377	404	422
La	mg/kg	12	11	14	12	20	21	25	14	11	9.9	11	15	14	17	22	17	16	16	19	18	25
Ce	mg/kg	22	22	27	26	39	40	48	25	21	20	22	29	26	32	45	35	33	32	39	36	50
Pr	mg/kg	3.0	2.6	3.0	2.8	4.6	4.9	5.9	3.4	2.7	2.4	2.7	3.8	3.4	4.1	5.2	4.0	3.7	4.0	4.8	4.6	6.4
Nd	mg/kg	10	9.2	10	9.9	17	18	21	12	9.9	8.5	9.5	13	12	15	19	15	13	15	17	17	23
Sm	mg/kg	2.0	1.8	2.0	1.9	3.3	3.5	4.1	2.5	1.9	1.7	1.9	2.7	2.5	3.0	3.7	2.9	2.6	2.9	3.5	3.4	4.6
Eu	mg/kg	0.45	0.37	0.45	0.42	0.69	0.76	0.86	0.55	0.44	0.41	0.47	0.64	0.57	0.69	0.76	0.66	0.54	0.53	0.62	0.65	0.81
Gd	mg/kg	1.7	1.6	1.8	1.8	2.8	3.0	3.6	2.1	1.7	1.6	1.8	2.5	2.3	2.8	3.3	2.6	2.4	2.4	3.0	3.0	3.8
Tb	mg/kg	0.27	0.25	0.28	0.29	0.44	0.46	0.54	0.34	0.27	0.25	0.30	0.39	0.35	0.40	0.47	0.38	0.34	0.36	0.44	0.45	0.57
Dy	mg/kg	1.6	1.5	1.8	1.9	2.7	2.8	3.1	2.1	1.7	1.7	2.0	2.4	2.1	2.4	2.7	2.2	2.0	2.1	2.6	2.6	3.3
Ho	mg/kg	0.30	0.29	0.34	0.36	0.49	0.51	0.56	0.38	0.33	0.33	0.39	0.45	0.38	0.44	0.49	0.39	0.36	0.38	0.47	0.48	0.59
Er	mg/kg	1.0	0.99	1.2	1.2	1.6	1.7	1.8	1.3	1.1	1.1	1.3	1.5	1.3	1.4	1.6	1.3	1.2	1.2	1.5	1.6	1.9
Tm	mg/kg	0.16	0.17	0.20	0.20	0.26	0.26	0.29	0.20	0.18	0.18	0.22	0.24	0.19	0.22	0.26	0.20	0.19	0.20	0.24	0.25	0.30
Yb	mg/kg	1.1	1.1	1.3	1.4	1.7	1.7	1.9	1.3	1.2	1.2	1.6	1.6	1.3	1.4	1.7	1.3	1.2	1.3	1.6	1.7	2.0
Lu	mg/kg	0.18	0.18	0.22	0.22	0.29	0.29	0.30	0.21	0.19	0.20	0.25	0.26	0.20	0.21	0.26	0.20	0.19	0.21	0.26	0.27	0.32
Hf	mg/kg	1.9	2.1	2.4	2.2	2.8	2.9	2.9	1.9	1.7	1.9	2.0	2.3	1.8	1.6	2.7	1.8	2.0	2.4	3.2	4.1	4.2
Ta	mg/kg	0.56	0.57	0.89	0.71	1.0	0.99	1.0	0.45	0.43	0.53	0.53	0.76	0.45	0.47	0.94	0.84	1.1	1.5	1.3	1.3	1.4
Tl	mg/kg	0.55	0.57	0.62	0.61	0.64	0.63	0.67	0.41	0.40	0.45	0.42	0.43	0.30	0.35	0.70	0.72	0.76	0.72	0.74	0.75	0.81
Pb	mg/kg	16	17	22	20	54	28	33	15	14	15	18	27	20	28	36	34	31	34	35	34	38
Bi	mg/kg	0.26	0.26	0.33	0.29	0.44	0.52	0.59	0.19	0.18	0.18	0.22	0.30	0.26	0.36	0.63	0.51	0.48	0.59	0.68	0.80	0.98
Th	mg/kg	5.7	5.9	6.4	6.4	8.7	8.9	10	5.8	4.8	5.0	5.2	5.8	4.5	5.2	9.9	8.1	9.0	9.6	11	11	15
U	mg/kg	1.6	1.7	2.1	1.9	2.3	2.4	2.5	1.5	1.3	1.5	1.6	1.7	1.2	1.2	2.5	2.0	2.2	2.5	3.1	3.4	4.0

A: 1–2mm, B: 500–1000 μm, C: 250–500 μm, D: 125–250 μm, E: 63–125 μm, F: 32–63 μm, G: <32 μm

石灰岩が河川堆積物中の元素濃度に与える影響の低さについて
—秋吉地域の例—

太田充恒・南　雅代

要　旨

　地質調査総合センターは日本において，細粒砂（＜180 μm）を用いた全国規模の53元素濃度の地球化学図を作成してきた．河川堆積物中の元素濃度の空間分布は地質や鉱山の分布を忠実に反映している．しかし，石灰岩岩体は例外であり，河川堆積物中の元素濃度にほとんど影響を与えていない．そこで我々は，この理由を明らかにすべく，日本最大規模の石灰岩岩体である秋吉台から採取した河川堆積物中の元素濃度並びに鉱物組成を調べた．流域に石灰岩を含む地域で採取された細粒砂（＜180 μm）は，CaO濃度が高く，そのX線回折データには強い方解石のピークが存在した．堆積物中の元素濃度の粒径依存性を調べたところ，粒径が細かくなるほど方解石の存在度が高くなりかつCaO濃度も増加した．しかし，石灰岩が流域に70%を超える面積を占める試料が示すCaO濃度は，予想される値（~50 wt. %）に比べて，10–20 wt. %と非常に低い．この矛盾した結果は，石灰岩岩体は化学風化によって水に溶けやすいが，物理風化・削剥を受けにくい事によって説明できる．すなわち，石灰岩岩体から供給される砕屑粒子の供給量が他の岩体の供給量に比べ圧倒的に低い事を意味する．また，SrはCaとよく似た化学的挙動を示す事が期待されるにもかかわらず，一部の試料中のSr濃度はCaO濃度や方解石のピーク強度とは良い相関関係を示さなかった．これは，炭酸カルシウムに対して過飽和な水から、秋吉石灰岩とは異なるSr濃度を持つ方解石が形成され、河川系に供給されたことを意味する．